Supplementary Information

FeMn Layered Double Hydroxides: An Efficient Bifunctional Electrocatalyst towards Real-time Tracking of Cysteine in Whole Blood and Dopamine in Biological Samples

Muthaiah Annalakshmi[1], Sakthivel Kumaravel[1,2], Shen-Ming Chen[1]*, Tse-Wei Chen[3]

[1]Department of Chemical Engineering and Biotechnology, National Taipei University of Technology, Taipei 106, Taiwan, ROC.

[2]Institute of Biochemical and Biomedical Engineering, National Taipei University of Technology, Taipei 106, Taiwan.

[3]Department of Materials, Imperial College London, London, UK

Corresponding Author: *Shen Ming Chen

E-mail: smchen78@ms15.hinet.net

Results and Discussions

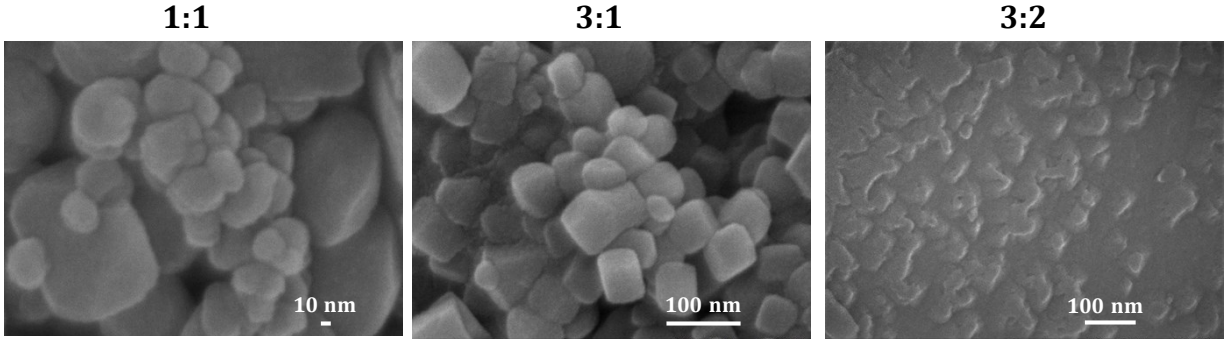

Fig S1. FESEM images of MnFe-LDH synthesized from different Mn : Fe molar ratios of precursors.

BET analysis

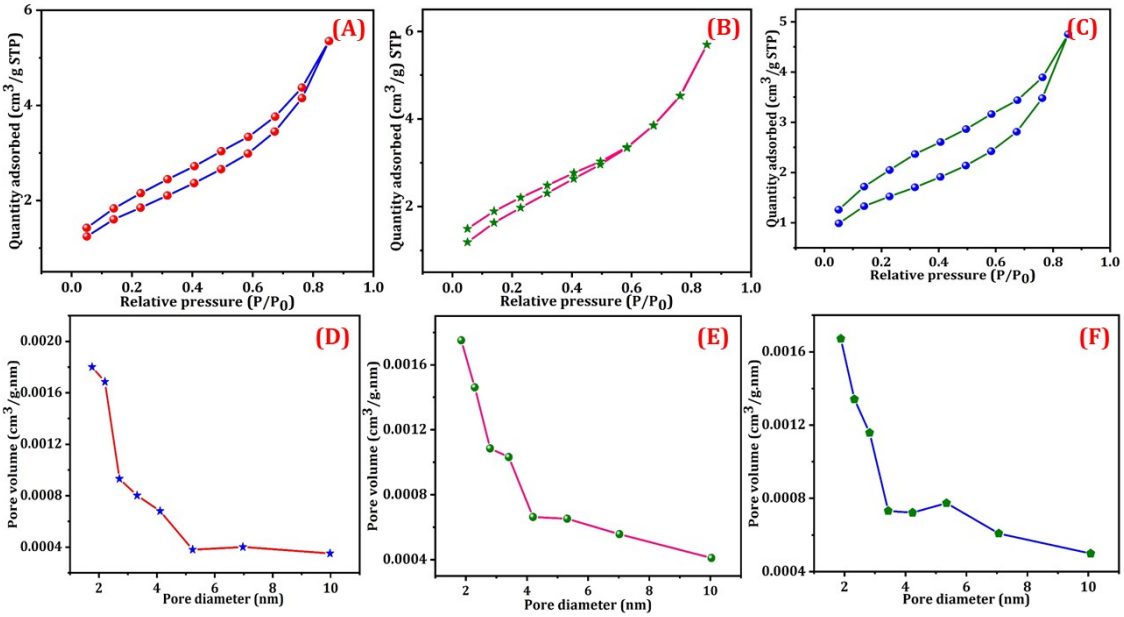

Fig. S2. N_2 adsorption and desorption isotherm (A-C) and pore size distribution profile (D-F) of FMH 6 h, 12 h and 18 h.

EDS analysis

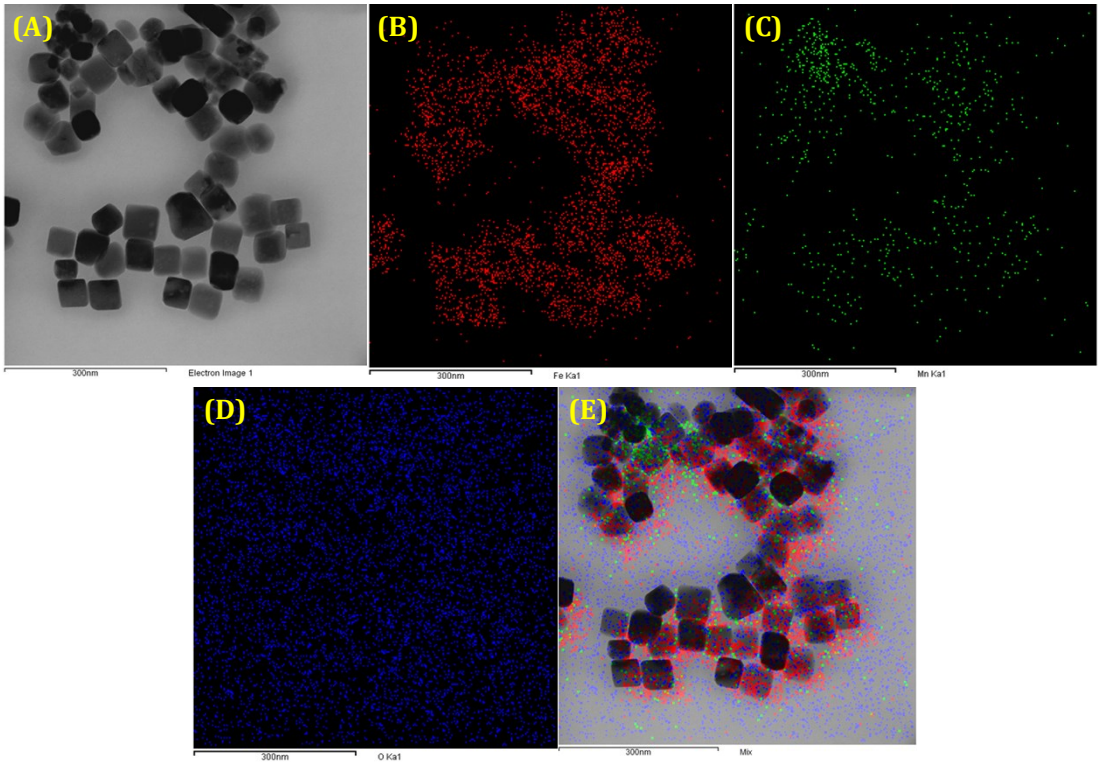

Fig. S3. (A-E) EDS elemental mapping of FMH, (B) Fe, (C) Mn, (D) O, and (E) Mix.

Loading amount of FMH on electrode surface

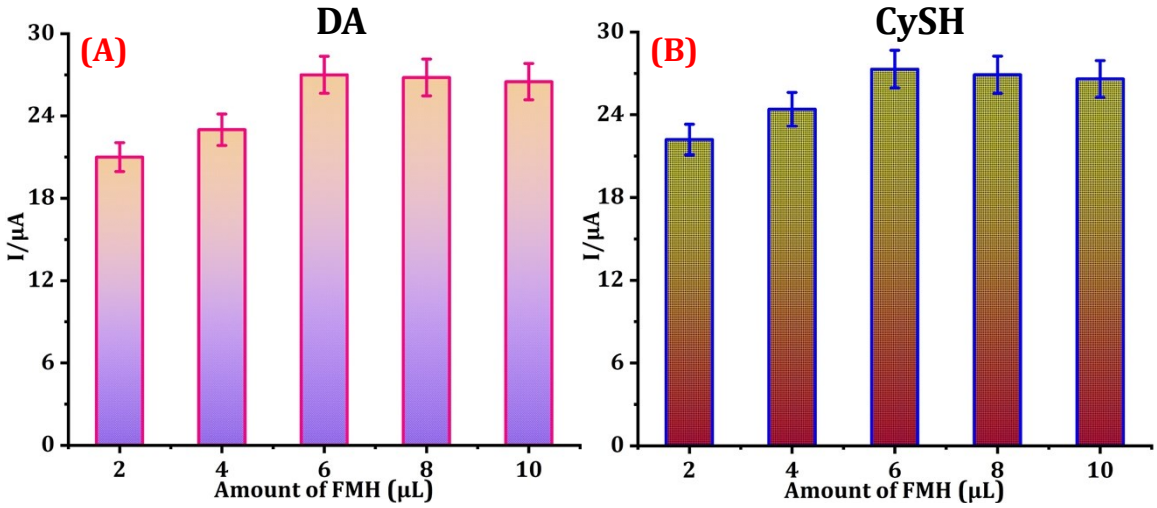

Fig. S4. (A) Anodic peak current response of various amount of FMH modified electrodes in the presence of 200 μA DA in 0.05 M PBS (pH 7). (B) Oxidation peak current response of various concentration of FMH/GCE toward 0.3 mM CySH in 0.05 M PBS (pH 7) (n=3).

The influence of pH on the electrochemical oxidation of DA and CySH

The influence of pH on the electrochemical detection of DA at FMH modified GCE was carefully studied by CV in wide range of pH from 3.0 to 11.0 (0.05 M PBS) and also, we analyzing the relationship between the anodic peak potential and the peak current. In general, the anodic peak current responses of DA increased with increasing the pH from 3.0 to 7.0 and reached maximum response current value at pH 7.0 (Fig. S5B). Further, increase in the pH from 7.0 to 11.0 resulted the gradual drop in the anodic peak current response as depicted in Fig. S5B. Moreover, their anodic peak potentials were shifted negatively as increasing the pH values (3.0-11.0), which is due to the deprotonation of the DA oxidation under the basic conditions. The linear plot of anodic peak potentials (E_{pa}) versus various pH solutions was presented in Fig. S5C, with a correlation coefficient value is R^2= 0.9972. The obtained slope value (52 mV) from the linear plot is close to the Nernstian theoretical value (59.1 mV/pH) at 25 °C, which confirms that the two protons/two electrons took part in the electrochemical oxidation reactions of DA, which is in agreement with previous reports.[1] Generally, the pKa value of DA is 8.72, which is basic, and explain it existence in a protonated form. According to the known formula pH=pKa + log ($[A^-]/[A]$), the pH of the solution is typically lower or higher than two units of pKa. So, the pH must be greater than two units of pKa for weakly acidic compounds to ensure completeness ionization. In the case of weakly basic compounds, the pH of the solution must be less than two units of pKa to ensure complete ionization which accounts the maximum response current at pH is 7.0, as most of the DA molecules exists in the ionized form at pH 7.0.

In addition, CySH contains pH-sensitive groups such as–NH_2, –COOH and –SH, therefore, the effect of pH solution on the electrocatalytic performance of FMH/GCE toward CySH oxidation was evaluated in the range from 5.0 to 9.0 in 0.05 M PBS by CV. As can be seen from Fig.S5E the anodic peak current is increased with the increasing of pH value from 5.0 to 7.0, afterwards, leads to decrease when the pH exceeded 7.0. Concomitantly, the peak

potentials shifted towards negative side as increasing the pH value from 5.0 to 9.0, indicating that the deprotonation involved in the oxidation process. Furthermore, the relationship between the oxidation peak potential and the peak current displays good linearity with a correlation coefficient (R^2=0.9907) (Fig.S5F). The maximum oxidation peak current is attained at neutral solution of pH 7, which is close to the physiological levels, and was chosen as the supporting electrolyte for subsequent experiments.

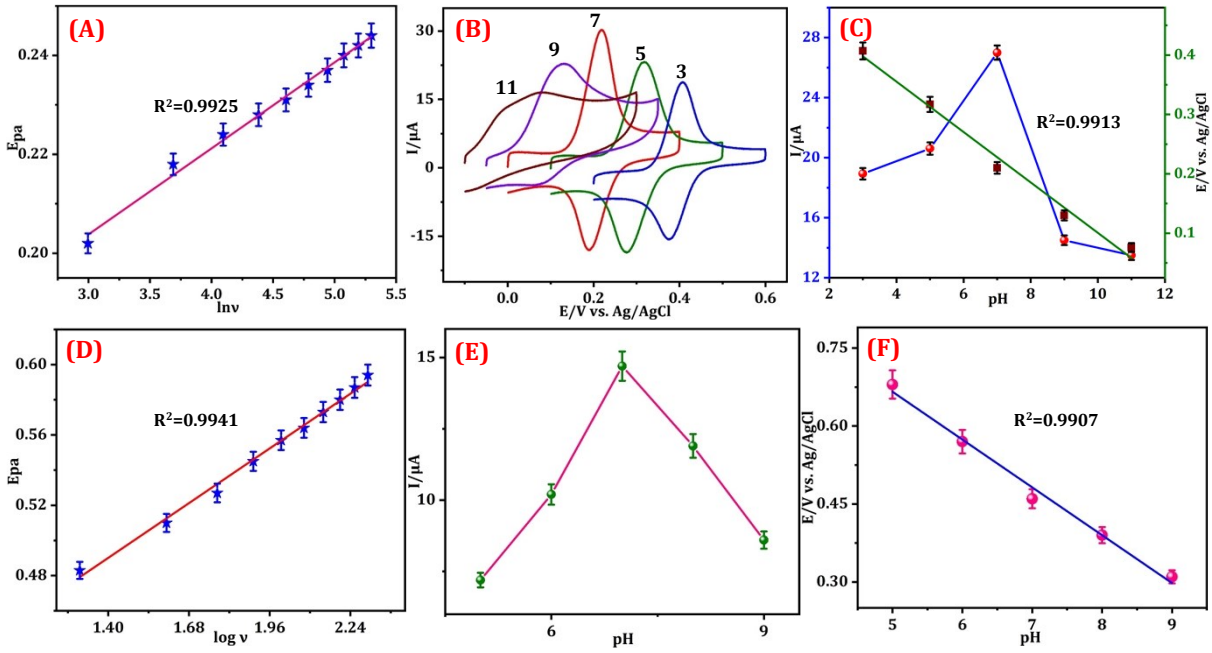

Fig. S5. (A) The linear plot amongst E_{pa} vs lnν. (B) CV responses of FMH/GCE toward 200 μM DA at a scan rate of 50 mV s^{-1} in various pH (0.05 M PBS) solutions (3, 5, 7, 9 and 11). (C) The calibration plot between the pH and anodic peak current (I_{pa}) (blue) and anodic peak potential (E_{pa}) (green) of DA. (D) Calibration plot between E_{pa} vs log ν toward CySH oxidation. (E) Effect of pH in the range from 5.0 to 9.0 (0.05 M PBS) vs oxidation peak current (I_{pa}) toward the electrooxidation of CySH. (F) Linear plot amongst oxidation peak potential (E_{pa}) and various pH.

Stability, reproducibility and repeatability of the developed sensor

The stability, repeatability, and reproducibility are the important factor for the real time applicability of an electrochemical sensor. The operational stability of FMH modified electrode was studied via amperometric technique towards 200 μM DA and 0.1 mM CySH in

0.05 M PBS (pH 7). As can be seen from Fig. S6A&D, the amperometric response current exhibits the retention current up to 97.76% and 98.79% from its initial after running time of 2000 s toward DA and CySH. To evaluate the storage stability of the sensor, the FMH/GCE was stored in room temperature over 25 days and the anodic peak current responses were monitored every five days toward 200 μM DA and 0.3 mM CySH in 0.05 M PBS (pH 7) were carried out by CV. As can be seen from inset of Fig. S6A and Fig. S6D, the sensor reveals only an accountable drop of 3.47 and 3.44 % from its initial current response on the 25th day, which indicates the excellent stability of the FMH modified electrode towards the detection of DA and CySH. This result implies that the FMH modified electrode had good operational and storage stability, which may ascribe to the unique morphology of nanocubes and greater number of active sites. Then the nanocubes were formed uniformly without any agglomeration, thus could ensures the good surface coverage of the electrode. Next, the repeatability of FMH modified electrode was investigated by observing 200 μM DA and 0.3 mM CySH over an FMH/GCE for seven consecutive measurements then the calculated relative standard deviations (RSD) are about 1.12% and 1.36%, respectively, for 7 measurements (Fig. S6B&E). Then to evaluate the reproducibility, there are five different FMH modified electrode were developed separately and analyzed toward 0.3 mM Cys and 200 μM DA was shown in Fig. S6C&F. The relative standard deviation (RSD) are to be 2.95% and 2.58%, respectively, for the determination of CySH and DA. From these observations clearly proves that the proposed FMH based sensor own good reproducibility and repeatability.

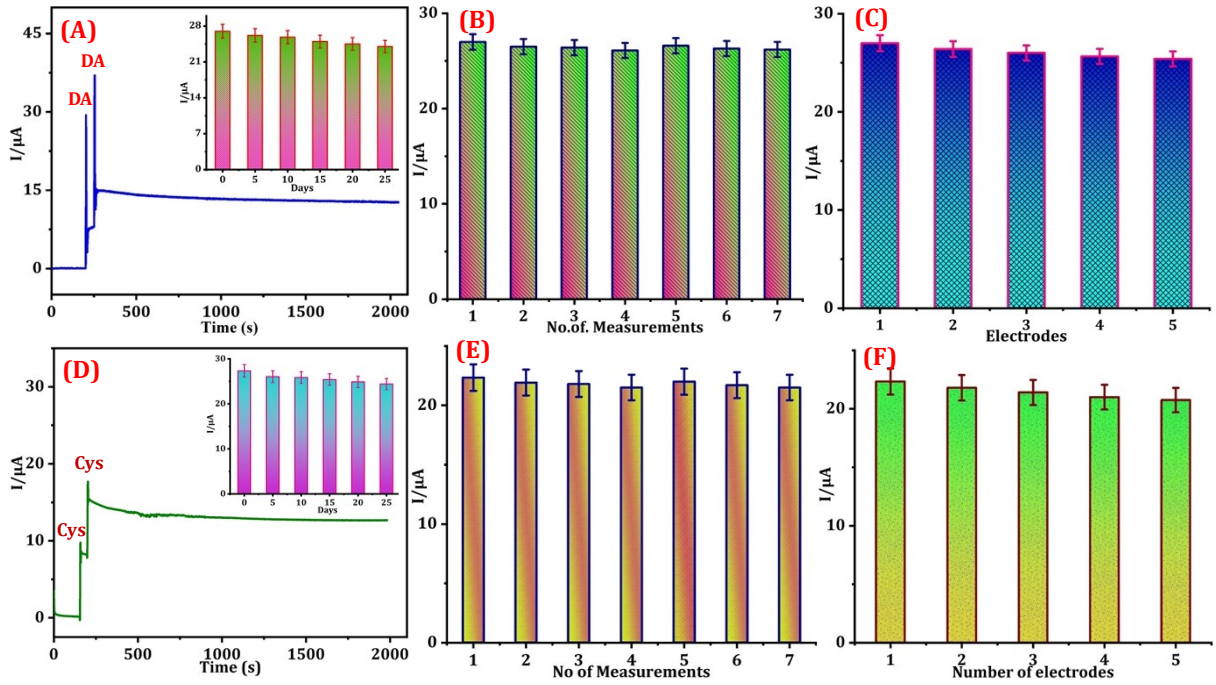

Fig. S6. (A) Operational and storage stability (inset) of FMH modified electrode toward 200 µM DA. (B) CV current response of FMH/GCE toward 200 µM DA for the seven consecutive measurements in 0.05 M PBS (pH 7) (n=3). (C) CV current response of five different NMH/GCE toward 200 µM DA in 0.05 M PBS (pH 7) (n=3). (D) Operational and storage stability (inset) of FMH modified electrode toward 0.3 mM CySH. (E) Reproducibility of the FMH modified electrode toward CySH oxidation. (F) Repeatability of the FMH modified electrode toward 0.3 mM CySH.

Table. S1. Comparison of analytical parameters of FMH modified electrode with several reported DA sensors.

Electrode	Technique	Linear range (μM)	LOD (μM)	Ref
Graphene/Diamond/GCE	DPV	5–200	200	[2]
Graphene/Pt/GCE	i-t	0.03–8.13	0.03	[3]
rGO/Co_3O_4/ GCE	i-t	0–30	0.277	[4]
Ag–Pt/pCNFs/ GCE	DPV	10–500	0.11	[5]
PABSA-rMoS_2/CPE	DPV	1–1000	0.22	[6]
CeO_2/Au-GCE	i-t	10–500	0.056	[7]
mMWCNT/SPE	SWV	5–180	0.43	[8]
ERGO/GCE	DPV	0.5–60	0.5	[9]
PANI/Au/ Nanoelectrode	DPV	0.3–200	0.1	[10]
CTAB/rGO/ZnS/GCE	DPV	1–500	0.5	[11]
ACCG/Nafion/GCE	i-t	0.1–50	0.1	[12]
CD-PNIPAM/GCE	DPV	0.1-60	0.0334	[13]
Au/polyaniline/GCE	i-t	3–115	0.8	[14]
N-doped graphene	DPV	0.5–170	0.25	[15]
FMH/GCE	i-t	0.02–700	0.0053	This work

rGO -reduced graphene oxide, pCNFs- Electrospun nanoporous carbon nanofibers, CNF-carbon nano fiber, PABSA-rMoS_2/CPE-poly (m-aminobenzenesulfonic acid)-reduced MoS_2/ carbon paste electrode, mMWCNT/SPE – magnetic multiwalled carbon nanotube/screen printed electrode, PANI-polyaniline, CTAB- cetyl trimethylammonium bromide, PA6/PAH-MWCNTs/ITO- polyamide 6/poly(allylamine hydrochloride-multiwalled carbon nano tubes nanofibers/indium tin oxide, MCNF/PGE- Mesoporous carbon nanofiber-modified pyrolytic graphite electrode.

Table S2. Comparison of analytical parameters of CySH over the several reported assays.

Electrode	Technique	Linear range (μM)	LOD (μM)	Ref
SWCNT arrayed-Pt	DPV	100	0.01	[16]
CNF-CPE	i-t	0.15–63.8	0.1	[17]
OMC-GCE	CA	18–2500	0.002	[18]
Cu/SPAuE	i-t	1–1800	0.21	[19]
GO-Au NCs/GCE	i-t	0.05–20	0.02	[20]
SnO_2-MWCNTs/GCE	i-t	0.1–554.5	0.03	[21]
CeO_2-CuO/GCE	CA	10–5000	0.016	[22]
MoS_2-Gr/GCE	DPV	0.01–1	0.02	[23]
Mg-Al-Ce LDH/GCE	i-t	10–5400	4.2	[24]
FMH/GCE	i-t	0.03–6666.7	0.0096	This work

CPE –carbon paste electrode; OMC-ordered mesoporous carbon; SPAuE-screen printed gold electrode; GO-Au NCs-graphene oxide gold nanoclusters;

References

1. Y. Wang, S. Wang, L. Tao, Q. Min, J. Xiang, Q. Wang, J. Xie, Y. Yue, S. Wu and X. Li, *Biosensors and Bioelectronics*, 2015, **65**, 31-38.
2. Q. Yuan, Y. Liu, C. Ye, H. Sun, D. Dai, Q. Wei, G. Lai, T. Wu, A. Yu and L. Fu, *Biosensors and Bioelectronics*, 2018, **111**, 117-123.
3. C.-L. Sun, H.-H. Lee, J.-M. Yang and C.-C. Wu, *Biosensors and Bioelectronics*, 2011, **26**, 3450-3455.
4. A. Numan, M. M. Shahid, F. S. Omar, K. Ramesh and S. Ramesh, *Sensors and Actuators B: Chemical*, 2017, **238**, 1043-1051.
5. Y. Huang, Y.-E. Miao, S. Ji, W. W. Tjiu and T. Liu, *ACS applied materials & interfaces*, 2014, **6**, 12449-12456.
6. T. Yang, H. Chen, C. Jing, S. Luo, W. Li and K. Jiao, *Sensors and Actuators B: Chemical*, 2017, **249**, 451-457.
7. Y. Tong, Z. Li, X. Lu, L. Yang, W. Sun, G. Nie, Z. Wang and C. Wang, *Electrochimica Acta*, 2013, **95**, 12-17.
8. Y.-M. Zhang, P.-L. Xu, Q. Zeng, Y.-M. Liu, X. Liao and M.-F. Hou, *Materials Science and Engineering: C*, 2017, **74**, 62-69.
9. L. Yang, D. Liu, J. Huang and T. You, *Sensors and Actuators B: Chemical*, 2014, **193**, 166-172.
10. Y. Zhang, L. Lin, Z. Feng, J. Zhou and Z. Lin, *Electrochimica Acta*, 2009, **55**, 265-270.
11. Y. J. Yang, *Sensors and Actuators B: Chemical*, 2015, **221**, 750-759.
12. A. Verma, S. Kumar, W.-K. Chang and Y.-P. Fu, *Dalton Transactions*, 2020, **49**, 625-637.
13. Y. Wu, Z. Dou, Y. Liu, G. Lv, T. Pu and X. He, *Rsc Advances*, 2013, **3**, 12726-12734.
14. A.-J. Wang, J.-J. Feng, Y.-F. Li, J.-L. Xi and W.-J. Dong, *Microchimica Acta*, 2010, **171**, 431-436.
15. Z.-H. Sheng, X.-Q. Zheng, J.-Y. Xu, W.-J. Bao, F.-B. Wang and X.-H. J. B. Xia, *Biosensors and Bioelectronics*, 2012, **34**, 125-131.
16. J. Okuno, K. Maehashi, K. Matsumoto, K. Kerman, Y. Takamura and E. J. E. c. Tamiya, *Electrochemistry communications*, 2007, **9**, 13-18.
17. X. Tang, Y. Liu, H. Hou and T. J. T. You, *Talanta*, 2010, **80**, 2182-2186.

18. M. Zhou, J. Ding, L.-p. Guo and Q.-k. J. A. C. Shang, *Analytical Chemistry*, 2007, **79**, 5328-5335.
19. A. Kurniawan, F. Kurniawan, F. Gunawan, S.-H. Chou and M.-J. J. E. A. Wang, *Electrochimica Acta*, 2019, **293**, 318-327.
20. S. Ge, M. Yan, J. Lu, M. Zhang, F. Yu, J. Yu, X. Song, and S. J. B. Yu, *Biosensors and Bioelectronics*, 2012, **31**, 49-54.
21. Y. Dong and J. J. J. o. M. L. Zheng, *Journal of Molecular Liquids*, 2014, **196**, 280-284.
22. G. Manibalan, G. Murugadoss, R. Thangamuthu, M. R. Kumar, R. M. Kumar and R. J. I. C. C. Jayavel, *Inorganic Chemistry Communications*, 2020, **113**, 107793.
23. K.-J. Huang, L. Wang, J. Li, and Y.-M. J. S. Liu, *Sensors and Actuators B: Chemical*, 2013, **178**, 671-677.
24. Y. Wang, W. Peng, L. Liu, F. Gao and M. J. E. a. Li, *Electrochimica acta*, 2012, **70**, 193-198.